Zagami: Product of a two-stage magmatic history

Timothy J. McCoy, G. Jeffrey Taylor, and Klaus Keil

Planetary Geosciences, Department of Geology and Geophysics, School of Ocean and Earth Science and Technology,
University of Hawaii at Manoa, Honolulu, HI 96822, USA

Abstract—Large specimens of the Zagami shergottite show highly varied grain sizes and mineral abundances on a cm scale and preferred alignment of pyroxene laths. We document the presence of whitlockite and of melt veins and pockets of shock origin. Pyroxene crystals have homogeneous Mg-rich pigeonite and augite cores, overgrown by Fe-rich, zoned pyroxene (mostly pigeonite) rims. Amphibole-bearing magmatic (melt) inclusions occur exclusively in the cores. We conclude that Zagami experienced a two-stage crystallization history. The first stage occurred in a deep-seated, slowly cooling magma chamber. There, the homogeneous Mg-rich cores of the pyroxenes crystallized during relatively slow cooling. The deep-seated origin of the cores is also indicated by the presence of amphibole within them, which requires pressures of formation equivalent to crystallization at depths > 7.5 km on Mars. Modest abundance of homogeneous Mg-rich cores (15–20%) indicates that crystal settling did not play a significant role in this part of the magma chamber. During the second stage, the Mg-rich pyroxenes were entrained into a magma that either intruded to the near-surface and cooled in a relatively thin dike or sill, or extruded to the surface and crystallized in a lava flow > 10 m thick, again without indications for crystal settling. This scenario is suggested by estimates of cooling rates of 0.1–0.5°C/h, based on sizes of the plagioclase (maskelynite) crystals, and of ~0.02°C/h, based on the width of pyroxene exsolution lamellae (Brearley, 1991). Irregular shapes of the Mg-rich cores result from resorption and possible solid-state diffusion, and the shapes and sizes of the pyroxenes after crystallization of Fe-rich pigeonite rims onto the cores were strongly controlled by the shapes and sizes of the cores. The finer-grained areas of the rock inherited smaller and more numerous Mg-rich pyroxene cores from the first stage than did the coarser-grained areas. Crystallization of both augite and pigeonite cores at depth, but mostly pigeonite rims in the near-surface environment, may be the result of a phase-boundary shift and expansion of the pigeonite stability field at lower pressures. The estimated depth of the magma chamber for Zagami of >7.5 km and thickness of the putative lava flow of >10 m are consistent with calculations and observations of volcanic constructs and flows in the Tharsis region of Mars.

INTRODUCTION

Studies of the SNC (Shergottites, Nakhlites, Chassignite) meteorites, which are thought to be impact ejecta from the planet Mars, have contributed significantly to understanding of the igneous history of the planet. The nine SNCs are petrologically diverse, ranging from basalts (shergottites) to pyroxenites (nakhlites) to a nearly monomineralic dunite (Chassigny). The five shergottites include the remarkably similar meteorites Shergotty and Zagami, the layered meteorite Elephant Moraine A79001, and the related harzburgites Allan Hills A77005 and Lewis Cliff 88516 (Antarctic Meteorite Newsletter, 1991). A sixth meteorite originally classified as a shergottite (Allan Hills A81313; 0.5 g) has been reclassified as a eucrite (Delaney and Prinz, 1989; H. Y. McSween Jr., pers. comm., 1991).

Among the SNCs, the shergottites have probably received the most attention, largely because of their drastically different ages obtained by different isotopic dating techniques and the effects that shock may have played in resetting these clocks. Isotopic age dating of mineral separates of shergottites by all techniques yields internal isochrons near 180 Ma, whereas a whole-rock isochron of four shergottites yields an age of 1.3 Ga. While the latter age is generally interpreted as the crystallization age of these rocks and the former as the age of the

shock event that converted the constituent plagioclase into maskelynite, alternative interpretations exist (e.g., Jones, 1986). Petrologic studies of the shergottites have documented extensive evidence for a major shock event in the history of these rocks (e.g., Stöffler et al., 1986).

Numerous petrologic studies of the shergottites have been carried out to unravel the crystallization histories of these enigmatic rocks, and different investigators have reached rather different conclusions. Most researchers conclude that crystal settling has played an important role in the igneous history of the shergottites (Duke, 1968; Smith and Hervig, 1979; Stolper and McSween, 1979; Grimm and McSween, 1982; McSween, 1985; Jagoutz and Wänke, 1986). A number of authors suggested that the shergottites experienced a one-stage crystallization history (Treiman and Sutton, 1991) and formed either as shallow intrusives (Duke, 1968; Treiman, 1985) or at depth in a magma chamber (Stolper and McSween, 1979; Jagoutz and Wänke, 1986); Brearley (1991) comments that Zagami formed in a shallow intrusive or, possibly, in a lava flow significantly thicker than 10 m. Other investigators propose a two-stage igneous history for the shergottites involving crystallization of the homogeneous, Mg-rich pyroxene cores in a magma chamber and of the Fe-rich, zoned overgrowths on these cores, as well as of the remainder of the rocks in

shallow intrusives (SMITH and HERVIG, 1979; MCSWEEN, 1985), perhaps up to 1 km in thickness (GRIMM and MCSWEEN, 1982).

We report the results of detailed studies of large specimens of the Zagami shergottite which we conducted as part of a consortium effort on new samples of this meteorite.

ANALYTICAL TECHNIQUES

We studied polished thin sections UNM 991 and 992 of the fine-grained pieces and UNM 993 and 994 of the coarse-grained pieces. Quantitative analyses of pyroxene, whitlockite, and shock melt were performed on a Cameca Camebax electron microprobe at an accelerating potential of 15 keV and an absorbed beam current of 20 nA on Rockport fayalite. Counting times of 20 sec were used. Differential matrix effects were corrected using ZAF procedures. A 20 μm broad beam was used to analyze shock melts in order to minimize volatilization.

Backscattered electron (BSE) images were taken using an ISI SS-40 scanning electron microscope. Photomosaics of portions of thin sections UNM 991 (fine-grained) and UNM 994 (coarse-grained) were obtained, using many individual BSE images at 30× magnification. The finished photomosaic of a portion of thin section UNM 991 measures approximately 43 by 30 cm, and that of a portion of thin section UNM 994 measures 54 by 30 cm. Mapping of cores was conducted by hand on the photomosaics. Quantitative analyses of pyroxenes determined the existence of cores in numerous grains throughout the photomosaic area. Most cores (both their presence and extent) were outlined on overlays of the photomosaics by comparison with the contrast level of these measured cores. While this subjective assessment introduces some errors, we estimate that our volume determinations (both for the bulk rock and individual cores) are accurate to within ±5 vol%. The actual vol% of cores and their areas were measured from our core outlines using digital image processing. The identification of the cores as either Mg-rich augite or Mg-rich pigeonite was accomplished by semiquantitative electron microprobe analysis, using 1 sec counts on scalers calibrated on grains whose precise quantitative compositions were previously determined by conventional electron microprobe techniques.

RESULTS

The mineralogy and texture of Zagami has been described previously by a number of authors (e.g., SMITH and HERVIG, 1979; STOLPER and MCSWEEN, 1979). We will not repeat

their findings here but concentrate on our new observations and measurements. These new results were made possible by the extraordinarily large samples available to us for study, in contrast to the limited sample sizes available to previous workers.

Hand Sample Descriptions

The two pieces of Zagami that we obtained weighed 19.5 and 352 g. Based on macroscopic appearance, we labelled the larger specimen as fine-grained and the smaller piece as coarse-grained (Fig. 1) although the coarse-grained specimen has highly varied grain size, in places identical to the fine-grained specimen. The larger piece is roughly cubic, 5 cm on a side, and is covered on one side by black shiny fusion crust and on five sides by saw cuts. Dark brown, glassy shock veins cut across this specimen. The smaller piece is a sawn slab, 5 × 3 × 0.4 cm, and contains glassy pockets.

Texture, Grain Size, and Mode

In order to determine the absolute grain sizes and the alignment of the constituent minerals more quantitatively, we measured four thin sections using the method of DAROT (1973), as employed by STOLPER and MCSWEEN (1979) in their study of Shergotty and Zagami. As discussed by these authors, quantitative petrofabric data on shergottites are difficult to obtain because of the existence of two clinopyroxenes with different optical orientations and the conversion of plagioclase to isotropic maskelynite. However, the technique of DAROT (1973) allows an estimate of the degree of alignment of these minerals by counting the number of grain contacts encountered during traverses at various angles to the apparent plane of foliation. Minima and maxima in the number of grain contacts correspond to the apparent plane of foliation and to the plane perpendicular to it, respectively.

Both thin sections of the fine-grained sample have a pronounced alignment of pyroxenes and maskelynite (Fig. 2), whereas section UNM 993 of the coarse-grained sample has

## FINE-GRAINED PIECE   COARSE-GRAINED PIECE

FIG. 1. Photographs of the fine- and coarse-grained pieces of Zagami (note slightly different scale) showing the faces that were cut for the consortium study. Shock vein material and strong preferential alignment of white pyroxene laths can be observed in the fine-grained piece. The coarse-grained piece shows no preferential alignment and marked variations in grain size.
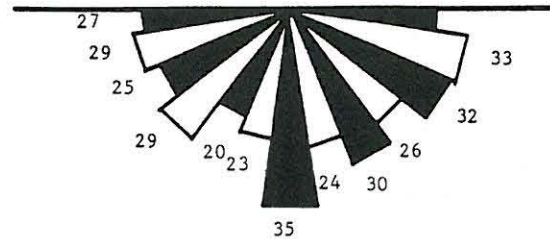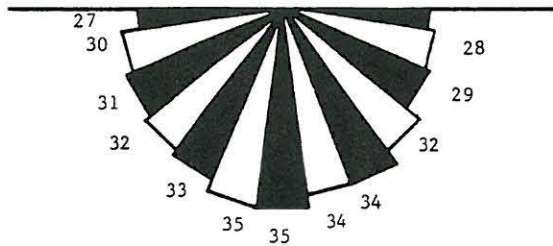
FINE-GRAINED SPECIMEN

UNM 991
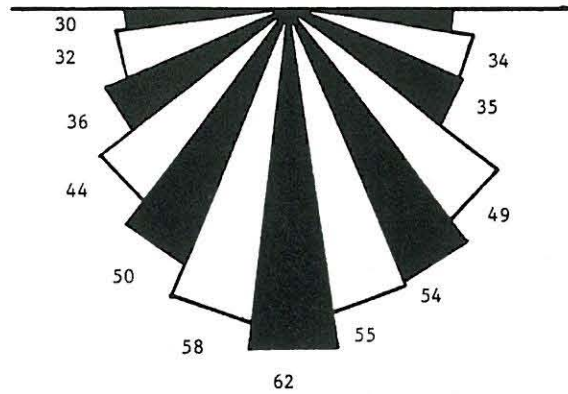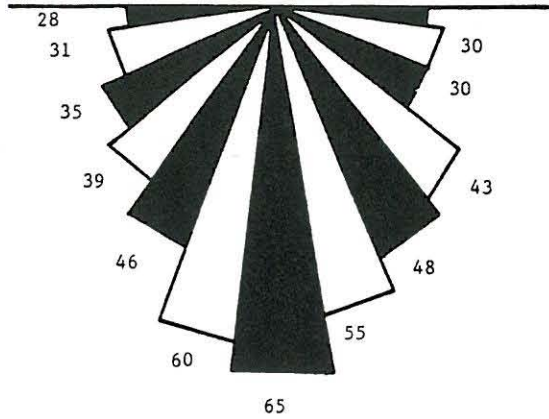
Average Grain Size = 0.24 mm

UNM 992

Average Grain Size = 0.22 mm

COARSE-GRAINED SPECIMEN

UNM 993

Average Grain Size = 0.19 mm

UNM 994

Average Grain Size = 0.36 mm

Plane of Foliation

FIG. 2. Sector diagrams for the fine- and coarse-grained specimens. Numbers indicate the number of grain boundaries crossed by traverses oriented at 15-degree angles. The minimum number of grain boundaries corresponds to the plane of foliation. The average grain size is equal to the total distance of all traverses divided by the number of grain boundaries. The fine-grained piece shows a strong preferred orientation and a relatively uniform small grain size. The coarse-grained specimen shows weak to no preferential alignment of pyroxene and variable grain size, including one area represented by section UNM 993 that is actually finer grained than the fine-grained hand specimen.

only a barely noticeable alignment and section UNM 994 has none. The differences in grain sizes between the two specimens are equally striking: The two thin sections of the fine-grained sample show nearly identical small average grain sizes (0.24 mm vs. 0.22 mm). In contrast, the grain size of thin section UNM 994 of the macroscopically coarse-grained hand specimen is indeed much coarser grained (0.36 mm), whereas thin section UNM 993 of the coarse-grained sample actually has smaller grain size (0.19 mm) than the fine-grained material; this thin section is clearly of fine-grained material. On an even larger scale, photos of the piece in the possession of R. Haag (16 × 17 × 6 cm), from which our samples were cut, also show highly variable grain sizes across all cut faces. In contrast to Elephant Moraine A79001 (MCSWEEN and JAROSEWICH, 1983), Zagami contain no sharp contact between fine- and coarse-grained material.

We also determined the modal abundances of minerals in the fine- and coarse-grained portions (Table 1). Thin sections of the fine-grained material (UNM 991, 992, 993) all have mineral abundances similar to those reported by STOLPER and MCSWEEN (1979), except that we find slightly higher pyroxene and slightly lower maskelynite contents; we attach no special significance to these minor differences. We also found significant amounts of whitlockite and shock-melted material not reported by previous investigators. However, the coarse portion of the rock, as represented by thin section UNM 994, has significantly different modal mineral abundances (Table 1): The total pyroxene content is significantly higher, and that of maskelynite is approximately 8 vol% lower; and the contents of minor phases are also somewhat higher than in the fine-grained portions.

Pyroxene Compositions and Abundances

Compositions of pyroxenes in the samples studied here are essentially identical to those reported by STOLPER and MCSWEEN (1979), except that the highest Fs contents we measured in the rims of pigeonite grains are slightly higher ($Fs_{54.3}$) than those measured by STOLPER and MCSWEEN (1979) ($\sim Fs_{48}$). Our values approach the highest Fs contents of pigeonite rims measured by these authors in Shergotty ($\sim Fs_{58}$).

As first noted by STOLPER and MCSWEEN (1979), pyroxenes often contain homogeneous Mg cores. In BSE imaging, a pigeonite grain from the coarse-grained material (Fig. 3) displays a prominent homogeneous Mg core. The homogeneity of the core is shown in the zoning profile. Although no distinct compositional break occurs between the core and the rim, the sharp zoning in the rim contrasts strongly with the core, allowing cores to be readily identified in BSE images. This core contains two magmatic inclusions, one of which is amphibole-bearing (in the following text). A slight increase in the iron content of the pyroxene surrounding the magmatic inclusion can be discerned.

Backscattered electron image mosaics of polished thin sections (Fig. 4) were used to determine the abundances, sizes, and shapes of the Mg-rich cores in fine- and coarse-grained samples (Fig. 5). Homogeneous Mg-rich cores are only slightly less abundant in the coarse-grained sample (14.4 vol%) than in the fine-grained sample (18.8 vol%). Their average maximum dimensions are 0.55 mm for the coarse-grained and 0.41 mm for the fine-grained areas. However, the Mg-rich cores in the fine-grained specimen are significantly smaller in area on average (0.057 mm^2) than those in the coarse-grained specimen (0.102 mm^2). The fine-grained sample contains more than twice as many cores as the coarse-grained sample, explaining the similarities in total abundances of the cores. The cores are either laths or spheres. Both the final shape of the individual pyroxene and the average grain size of the rock are strongly controlled by the shapes and sizes of the homogeneous Mg cores.

We also determined the compositions of a significant number of Mg-rich cores in both the fine- and coarse-grained samples to determine the relative abundances of augite vs. pigeonite cores. We find that augite cores are more abundant than pigeonite cores and that the ratio of the number of augite to pigeonite crystals is 1.5 in the fine-grained and 2.2 in the coarse-grained rock. In both the fine- and coarse-grained material, the average pigeonite cores are larger than the average augite cores: in the fine-grained material, the augite cores are 0.053 mm^2 in area and the pigeonite cores are 0.088 mm^2; whereas in the coarse-grained material, the augite cores measure 0.092 mm^2 and the pigeonite cores 0.166 mm^2. In contrast, the compositions of the Fe-rich rims on Mg-rich cores

Table 1.   Modal analysis of fine- and coarse-grained portions of Zagami, compared with data from STOLPER AND MCSWEEN (1979).

| Mineral	Fine-Grained Specimen		Coarse-Grained Specimen		STOLPER AND MCSWEEN
	UNM 991	UNM 992	UNM 993	UNM 994	BMNH 1966,54
Pyroxene	77.7	74.3	76.0	80.4	
Augite					36.5
Pigeonite					36.5
Maskelynite	17.6	18.8	18.6	10.3	21.7
Mesostasis	1.8	3.0	2.1	3.7	2.1
Oxides	1.5	1.8	2.0	2.6	2.1
Titanomagnetite					
Ilmenite					
Pyrrhotite	0.6	0.4	0.4	0.6	trace
Whitlockite	0.5	0.6	0.5	1.3	trace
Shock Melts	0.1	0.9	0.3	0.9	none
No. of Points	2000	2000	2000	2000	
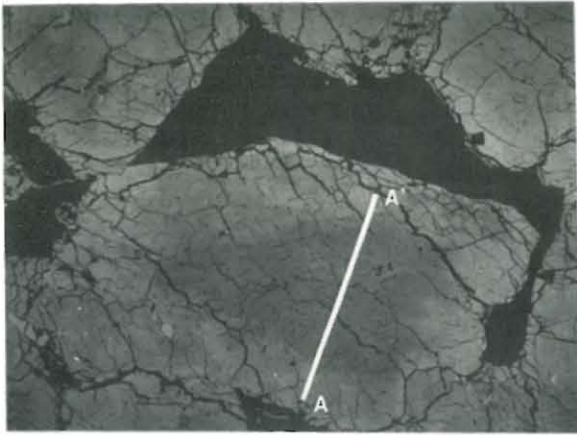
Pigeonite Zoning
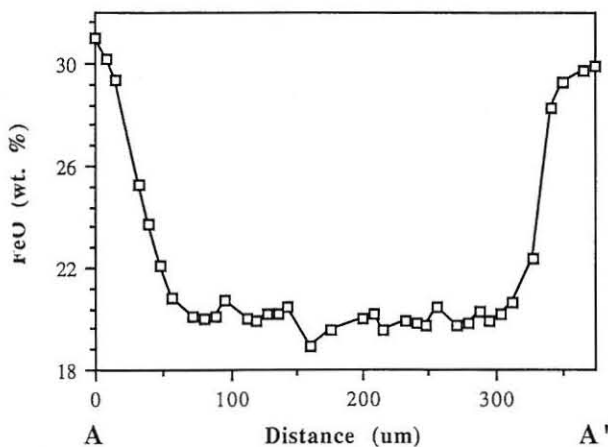
FIG. 3. Backscattered electron image of a pigeonite grain from the coarse-grained portion (UNM 994), with a zoning profile from A to A'. This grain displays a prominent homogeneous Mg core with a zoned, Fe-rich rim. Two magmatic inclusions (black areas just to right of zoning profile) are evident with some small enrichment of Fe around the inclusions. One of these inclusions is amphibole-bearing.

indicate a ratio of pigeonite to augite of 12.3 in the coarse-grained material (we did not determine this ratio for the fine-grained specimen).

Amphibole-bearing Melt Inclusions

TREIMAN (1985) first identified kaersutitic, water-bearing amphibole in melt inclusions in pyroxenes of Zagami, often associated with spinel. We conducted a random microscopic survey of areas of polished thin sections from which homogeneous Mg-rich cores had been previously mapped. In the fine-grained portions of the rock, we were able to confidently identify amphibole by its color and pleochroism in eight melt inclusions. These inclusions range in size from 10–40 μm in diameter, and all eight (contained in a total of five cores) are present in homogeneous Mg-rich pyroxene cores. Four additional inclusions in Mg-rich pyroxene cores probably also contain amphiboles, but because of their locations below the surface of the thin section, amphibole could not be positively

identified. Finally, two spinel-bearing inclusions were noted in Mg-rich cores, but they do not appear to contain amphibole.

In the coarse-grained portions of the rock, two melt inclusions were observed in which amphibole is on the surface of the section and could be positively identified. These inclusions also occur in a Mg-rich pyroxene core. Nine other melt inclusions in Mg-rich cores almost certainly contain amphibole; but the inclusions are not on the surface of the section, and amphibole could not be identified with confidence. Furthermore, a single spinel-bearing inclusion was found and it also occurs in the core of a pyroxene. We conclude that amphibole-bearing melt inclusions in the fine- and coarse-grained lithologies occur exclusively in the homogeneous, Mg-rich cores.

Whitlockite

Whitlockite has not previously been identified in Zagami, but we find its properties to be nearly identical to that in Shergotty (e.g., FUCHS, 1969; STOLPER and MCSWEEN, 1979; SMITH and HERVIG, 1979; JAGOUTZ and WÄNKE, 1986). The mineral occurs interstitially in large, hexagonal crystals (>200 μm), much like whitlockite from Shergotty (Fig. 8f in STOLPER and MCSWEEN, 1979). No significant compositional differences are noted in whitlockite in the fine- and coarse-grained material. Its average composition corresponds
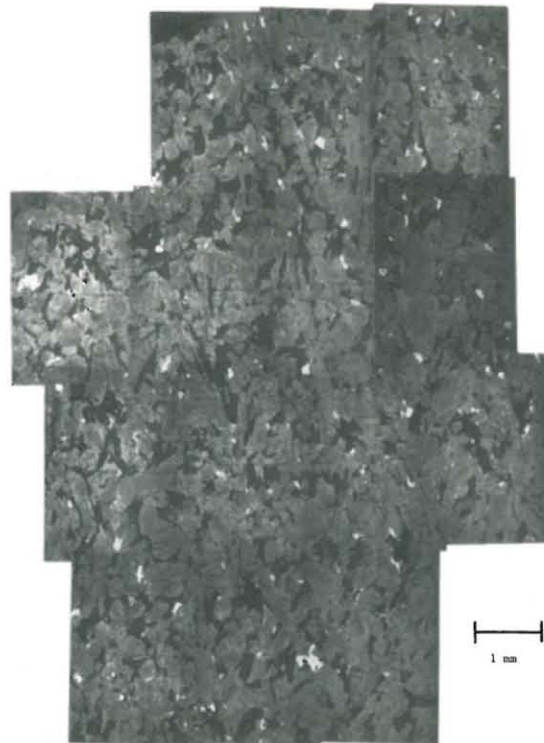

FIG. 4. Photomosaic of individual BSE images of a portion of polished thin section UNM 991, the fine-grained material. White = oxides and sulfides; black = maskelynite. Pyroxenes are zoned with darker, homogeneous Mg-rich (i.e., Fe-poor) cores and lighter, zoned Fe-rich rims. Scale bar equals 1 mm.

FINE-GRAINED MATERIAL   **COARSE-GRAINED MATERIAL**
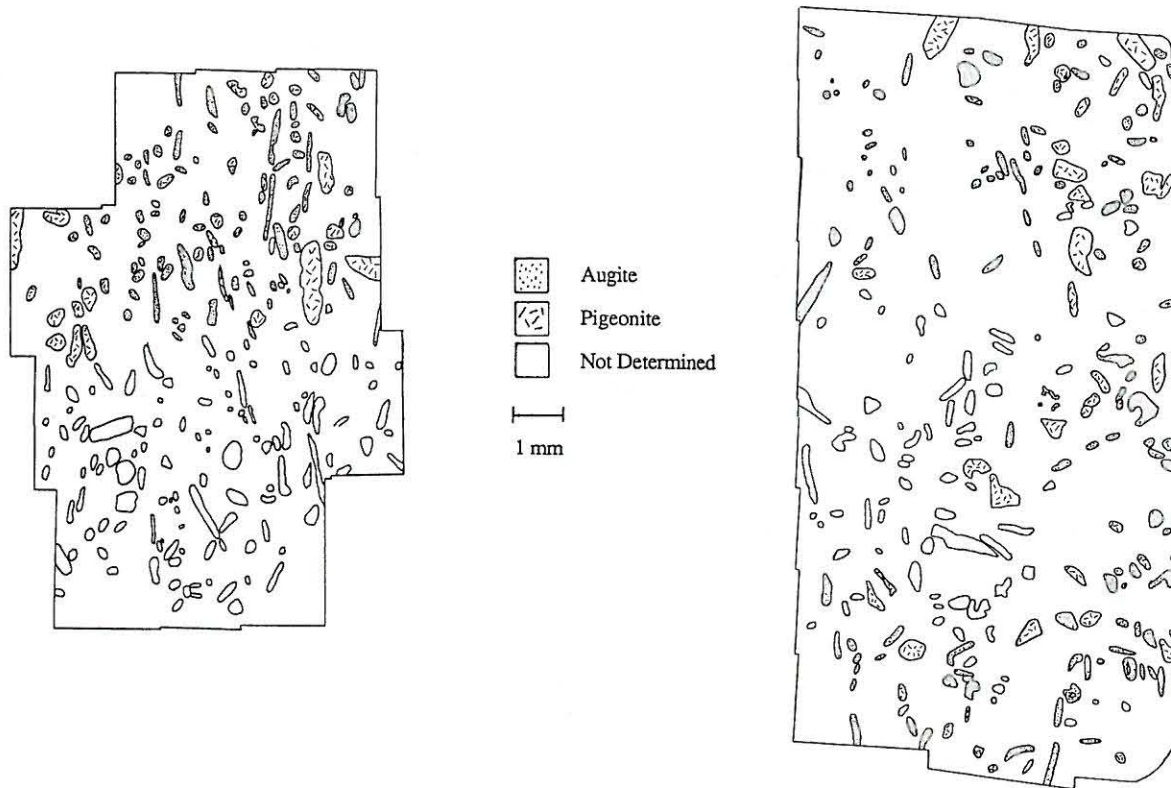

FIG. 5. Homogeneous Mg-rich cores mapped from BSE image photomosaics of the fine-grained (UNM 991) and the coarse-grained (UNM 994) material. Maps are to the same scale; and cores are mapped as augite, pigeonite, or not determined. The abundances are roughly similar (14.4 vol% in the coarse- and 18.8 vol% in the fine-grained material), but the average area of fine-grained cores is about half the area of coarse-grained cores (i.e., the former contains about twice as many cores than the latter).

to a structural formula of $Ca_{2.64}Fe_{0.13}Mg_{0.17}Na_{0.11}$ $(P_{1.0}O_4)_2$, which is nearly identical to that of whitlockite in Shergotty. We did not identify chlorapatite in Zagami, which has been observed in Shergotty (FUCHS, 1969; SMITH and HERVIG, 1979).

As reported by STOLPER and MCSWEEN (1979) for Shergotty, whitlockites often contain elongated glass inclusions. A common feature of the inclusions is that opaque phases occur at one end, suggesting that gravitational settling is responsible for their location. The direction of settling was consistently normal to the apparent plane of foliation, based on observations of a small number of glass inclusions (H. Y. McSween Jr., pers. comm., 1991). We have also observed opaque phases in glass inclusions within whitlockite crystals from Zagami which, in many cases, appear on one end of the inclusions. However, the apparent direction of "settling" is not consistent from inclusion to inclusion, and some inclusions have opaque phases that nucleated all around their boundaries. We conclude that the occurrence of the opaque phases did not result from gravitational settling but may have been affected by other processes (e.g., surface tension).

Shock Melts

The shergottites, including Zagami, are the most highly shocked of the SNC meteorites and are characterized by the presence of maskelynite rather than crystalline plagioclase. As part of the Zagami Consortium, a detailed study of the rock's shock features has been carried out by LANGENHORST et al. (1991); and here, we discuss only briefly shock melts and pockets which we discovered in hand specimens and thin sections.

Shock-melted material occurs in two textural types in Zagami, as veins and as pockets. Veins occur in the fine-grained sample (Fig. 1) and range from a few to several hundred μm in width and span the entire fine-grained piece. These veins seem to follow the preferred alignment of the pyroxene laths. Broad-beam electron microprobe analyses show that the veins are fairly homogeneous and similar in composition to bulk Zagami. Slight enrichments of SiO_2, Al_2O_3, and Na_2O, along with depletions of FeO and MgO, relative to the bulk composition, suggest that the veins may have incorporated plagioclase in greater than modal proportions, as also observed

in shock melts of Elephant Moraine A79001 (McSween and Jarosewich, 1983).

Localized melt pockets occur in both the fine- and coarse-grained samples. In some instances, melt pockets may be shock veins cut in cross section by the plane of the thin section, as indicated by bulk compositions which are very similar to bulk Zagami. However, others appear to be pockets of localized melting, as suggested by their bulk compositions, which are unlike bulk Zagami. One pocket, for example, appears to have large proportions of pigeonite in the melt, whereas two others seem to reflect preferential localized melting of phosphates.

DISCUSSION

We suggest that the mineralogical composition and texture of the shergottite Zagami can be explained best by a two-stage crystallization history.

Two-stage Magmatic History

Three lines of evidence (discussed in detail later) point to the need for a two-stage magmatic history. The zoned, Fe-rich rims on homogeneous, Mg-rich cores of pyroxenes imply slow cooling during core formation followed by rapid crystallization during rim crystallization. The presence of pigeonite rims on augite cores suggests an interruption of the crystallization of the pyroxenes. Finally, the location of amphibole-bearing melt inclusions exclusively in the cores of the pyroxene grains implies high-pressure crystallization of the cores and low-pressure crystallization of the Fe-rich rims. Together, these lines of evidence require a two-stage magmatic history with slow-cooling at depth and rapid cooling at or near the surface, with a hiatus between the two stages.

Some authors would argue that the presence of cores does not require a two-stage magmatic history. As noted by Pearce (1987), random sectioning through normally zoned grains can yield the appearance of homogeneous (or nearly so) cores. However, the presence of pigeonite rims on augite cores suggests that homogeneous Mg cores in Zagami are not an artifact of sectioning. A variety of physical histories can be envisaged to satisfy the need for a two-stage magmatic history. Although none of these can be rigorously excluded, they all suffer from one or more serious problems. It is possible that the cores are xenocrysts, unrelated to the remainder of Zagami. Stolper and McSween (1979) note that both the augite and pigeonite cores appear to have equilibrated with magmas of $Fe^{2+}/(Fe^{2+} + Mg)$ ratio of 0.64–0.67, strongly suggesting co-precipitation. This magma could have been the intercumulus liquid enriched in Fe during core crystallization, and there is no reason to invoke a xenocrystic origin for the cores in Zagami. Further, if the xenocrysts are from a partially digested wall rock, all phases except the pyroxenes would have to be resorbed. While this cannot be excluded, it does present some problems. A second alternative is that the cores crystallized during magma ascent with the rest of the rock crystallizing at or near the surface. However, it appears that a critical change in both pressure and cooling rate occurs at the core-rim boundary in the pyroxenes. We see no reason to believe

that a slowly ascending magma would cross the critical pressure for amphibole crystallization (1 kbar) at the same level at which cooling rate changes dramatically. Instead, a rather catastrophic change in the environment must occur during pyroxene crystallization. Impact would provide such a catastrophic change with excavation of a slowly cooling deep-seated magma body. Again, this cannot be rigorously excluded, but it is clear that more conventional means (e.g., eruption) exist to bring a magma to the surface.

We believe that the following scenario is consistent with the petrology of Zagami, as well as with inferences about the geology of Mars. In the first stage, the homogeneous Mg-rich pyroxenes (augite and pigeonite) crystallized during relatively slow cooling at depth in a magma chamber, and amphibole crystallized in melt inclusions trapped in these pyroxenes because of elevated pressures at depth. In the second stage, these pyroxenes became entrained in a melt that was transported to the near-surface and cooled as a relatively thin intrusion, or erupted at the surface and cooled as a thick lava flow. In this stage, the melt cooled relatively rapidly; the Mg-rich pyroxenes served as nucleation sites for overgrowths by zoned, Fe-rich pigeonite; and the rest of the rock crystallized. Crystal settling was not an important process in either stage.

Stage One: Magma Chamber

We propose, in agreement with earlier workers (e.g., Stolper and McSween, 1979; Smith and Hervig, 1979), that crystallization of phenocrysts in a deep-seated, slowly cooling magma chamber provides the most reasonable scenario for formation of the homogeneous Mg cores. However, uncertainties exist as to the sequence of crystallization of the pigeonite and augite cores. Pigeonite may have nucleated first, as suggested by the much larger sizes of the pigeonite relative to the augite cores. Alternatively, kinetic barriers or differences in growth rates could also explain this difference in grain size between pigeonite and augite cores, and size may not be related to time of nucleation.

We believe that the first magmatic stage occurred under significant pressure. Experiments by Gilbert et al. (1982) and Johnson et al. (1991) indicate that kaersutite crystallizes only under H_2O pressures in excess of 1 kbar in the presence of basaltic melt. Johnson et al. (1991) conclude that a maximum pressure cannot be confidently inferred, but all of the data available from their study of magmatic inclusions in Chassigny point to crystallization at pressures ≤ 5 kbar, possibly <2 kbar. Pressures of 1–2 kbar on Mars correspond to depths of 7.5–15 km, assuming terrestrial basalt-like densities. The occurrence of amphiboles exclusively in the homogeneous, Mg-rich pyroxene cores provides strong evidence that the cores formed at depth > 7.5 km in a magma chamber, whereas the remainder of the rock crystallized under low pressure.

Compatibility of magma chamber concept with Martian volcano constructs

Is the idea of core crystallization at depths of >7.5 km consistent with current knowledge of Martian volcano con-

structs and the depth of Martian magma chambers? The young ages of the SNC meteorites imply that they must come from a very young volcanic terrain on Mars. The only area on Mars with regionally extensive young volcanic units is Tharsis, making this the only reasonable candidate for the SNC parent terrain (e.g., MOUGINIS-MARK et al., 1992). ZUBER and MOUGINIS-MARK (1990) calculated a best-fit range for the depth to the Olympus Mons magma chamber of approximately 8–16 km, based on strain patterns observed in the caldera complex. Regrettably, calculations for other Tharsis volcanic constructs have not been performed, but the similarities in magma chamber depths implied by amphibole crystallization experiments (7.5–15 km) and strain rate calculations (8–16 km) for Olympus Mons suggest that the homogeneous Mg-rich pyroxene cores in Zagami crystallized in a "typical" Tharsis-type volcano magma chamber.

Potential role of crystal settling in the magmatic history of shergottites (stage one)

Several previous investigators have argued that gravitational crystal settling played an important role in the igneous history of the shergottites (DUKE, 1968; SMITH and HERVIG, 1979; STOLPER and McSWEEN, 1979; GRIMM and McSWEEN, 1982; McSWEEN, 1985; JAGOUTZ and WÄNKE, 1986). Both the accumulating phases and the time of accumulation have been debated. All authors have cited pyroxene as a cumulus phase, although it is uncertain whether accumulation was limited to the homogeneous Mg-rich cores (STOLPER and McSWEEN, 1979) or to the entire pyroxenes, after overgrowth of the Fe-rich rims (SMITH and HERVIG, 1979).

The abundance of homogeneous Mg-rich cores has been the strongest evidence for a cumulate origin of the shergottites. STOLPER and McSWEEN (1979) conducted a series of partial melting experiments on samples of Shergotty and Zagami to determine the abundances of the homogeneous Mg-rich cores. They found that Zagami contains 45% cores (23% augite, 22% pigeonite) (note that these authors combine their vol% modes and wt% chemical data, presumably because of the similar densities of the major phases concerned). This high abundance prompted them to conclude that gravitational settling in the magma chamber must have been an important process. Recent estimates by TREIMAN and SUTTON (1991) yield abundances of cores between 25–30%, using a mass balance of nickel. However, based on mapping of BSE images, we determined that the cores comprise only 15–20 vol% of Zagami. Thus, in light of the modest abundances of Mg-rich cores present in Zagami (15–20 vol%), we conclude that gravitational settling and accumulation of cores does not appear to have been an important process in the magmatic history of Zagami.

In order to further address the suggestion by others that crystal settling of pyroxene may have been important in the crystallization history of Zagami, we developed a computer program to evaluate the settling of pyroxene cores. This program uses Stokes' Law to calculate the total settling distance of a crystal of known size and density through a magma of known composition, crystal content, initial and final temperature, and cooling rate. In the case of Zagami, we used

an average pyroxene core radius of 0.1 mm, with a density of 3 g cm^{-3}. The composition of the intercumulus magma was taken as that of the bulk composition of Zagami (Table 2), minus 10 wt% each of augite and pigeonite of core compositions. The composition of this liquid is basaltic (~51 wt% SiO$_2$) and rich in FeO (~18.5 wt%). To calculate the density and viscosity of the magma, we used the programs given by McBIRNEY (1984), which are based on the methods of BOTTINGA and WEILL (1970) to calculate the density, and SHAW (1972) to calculate the viscosity of the magma. The effective viscosity of the magma was calculated using the relation $\eta_{eff} = \eta_0 (1-1.7\phi)^{-2.5}$. The value of 1.7 is given by McBIRNEY (1984) for natural magmas containing crystals of different sizes and shapes. For the crystal content of the magma, we used a value of 20% ($\phi = 0.2$); and the surface gravity of Mars was taken to be 372 cm s^{-2}. The actual calculation is carried out in a series of temperature steps, and the distances settled in each increment are added to calculate the total settling distance. This model is less sophisticated than that of GRIMM and McSWEEN (1982) but should provide basic insights into the feasibility of crystal settling during the formation of the shergottites.

We calculated a settling velocity for the homogeneous Mg-rich pyroxene cores in the magma chamber at 1150°C of 2.8 × 10^{-6} cm s^{-1}. This corresponds to a settling distance of 88 cm y^{-1}, or nearly one km per thousand years. This simple calculation suggests that crystal settling should, in fact, have been important over the expected extended lifetime of the magma chamber. However, these simple calculations ignore a number of very important effects which act in terrestrial magma chambers. Chief among these are convection, which would tend to disrupt the simple gravitation sinking of a crystal. In fact, individual crystals may not sink at all in real magma chambers but may require groups of crystals to begin gravitational segregation. Although Zagami does contain phenocrysts (the homogeneous cores of the pyroxenes) that formed in a deep magma chamber, these cores comprise only 15–20% of the rock. This is a relatively modest abundance and could have crystallized from the magma without segregation. Other parts of the magma chamber not sampled by known shergottites might have been affected by cumulate processes, but the mineralogy of Zagami has not been affected much by these processes.

Our results would seem to be in direct contradiction to the work of STOLPER and McSWEEN (1979). We have no real explanation for this discrepancy but offer several possibilities. The first of these is that these authors worked on Zagami samples from the British Museum, which could differ from the University of New Mexico samples. To the best of our knowledge, no individual has studied both sets of samples. However, our data suggests extreme similarities between these samples, and we see no reason to believe that sample heterogeneity could explain the differences in core abundances. A second alternative, originally suggested by STOLPER and McSWEEN (1979), is that their experiments did not accurately reproduce the early history of pyroxene crystallization in Zagami. These authors argued for pyroxene accumulation based on the fact that their first formed pyroxenes were more magnesian that natural pyroxenes in Zagami or Shergotty. To reproduce the natural core compositions, lower temper-

Table 2. Bulk composition, mineral and shock melt compositions, and calculated intercumulus magma composition (in wt. %) for Zagami.

	(1)	(2)	(3)	(4)	(5)	(6)	(7)	(8)	(9)	(10)
SiO$_2$	51.2	53.0 *0.86*	51.7 *1.04*	50.7	n.a.	51.8 *0.99*	52.6	50.9	43.4	44.0
Al$_2$O$_3$	6.19	0.78 *0.20*	1.20 *0.17*	7.8	n.a.	8.51 *1.54*	9.05	1.69	1.66	4.86
Cr$_2$O$_3$	n.a.	0.45 *0.11*	0.71 *0.04*	n.a.	n.a.	n.a.	n.a.	n.a.	n.a.	n.a.
TiO$_2$	0.81	0.15 *0.03*	0.22 *0.03*	1.03	n.a.	0.82 *0.23*	0.81	0.46	0.83	2.48
MgO	10.4	20.7 *0.92*	15.8 *0.71*	7.98	2.20 *0.15*	8.61 *1.48*	8.57	10.4	8.15	7.10
MnO	0.55	0.63 *0.04*	0.44 *0.05*	0.54	n.a.	0.51 *0.09*	0.53	0.81	0.57	0.33
FeO	18.2[†]	19.2 *0.76*	12.9 *1.02*	18.5	2.96 *0.25*	18.7 *1.53*	19.0	30.2	22.6	24.2
CaO	10.7	5.6 *1.07*	16.1 *0.60*	11.2	47.4 *0.47*	10.3 *1.43*	9.11	6.82	17.1	12.8
Na$_2$O	1.29	0.10 *0.04*	0.18 *0.01*	1.64	1.04 *0.09*	1.63 *0.36*	1.67	0.31	0.49	1.26
K$_2$O	0.13	n.a.	n.a.	0.18	n.a.	0.19 *0.65*	0.12	0.01	0.10	0.13
P$_2$O$_5$	0.58	n.a.	n.a.	0.71	45.6 *0.33*	0.65 *0.61*	0.14	0.04	6.18	3.99
Total	100.05	100.61	99.25	100.28	99.20	101.72	101.60	101.64	101.08	101.15
N		16	6		20	6	1	1	1	1

(1) Zagami bulk composition (P. NOLL, pers. comm., 1990) (2) Homogeneous Mg pigeonite cores (3) Homogeneous Mg augite cores (4) Calculated intercumulus magma (bulk - 10% each of augite and pigeonite cores) (5) Whitlockite (6) Shock melt vein (7) Shock melt pocket 1 (8) Shock melt pocket 2 (9) Shock melt pocket 3 (10) Shock melt pocket 4.

n.a. indicates non-analyzed elements.
Figures in italics are 1σ of N analyses.
Total iron reported as FeO.

atures and larger concentrations of cores were needed. However, they suggested, and subsequently rejected, the idea that early formed cores could have been more magnesian and would have homogenized with the Fe-rich liquid during slow cooling. Thus, the natural cores are now more Fe-rich than when they first crystallized. This idea is consistent with our model of core crystallization, in which early cores could homogenize with a more Fe-rich liquid during slow cooling in the deep-seated magma chamber. Although we cannot exclude other possibilities, this would explain the discrepancies between our modal core abundances and those observed by STOLPER and MCSWEEN (1979).

Stage Two: Shallow Intrusion or Lava Flow

After entrainment of the homogeneous Mg-rich cores, emplacement of the magma must have occurred as either a thin intrusion or thick lava flow, providing an environment for crystallization of the remainder of the rock during rapid cooling. Here, we examine the details of the second magmatic stage.

Previous arguments for formation in a shallow intrusion

Previous investigators have repeatedly cited the work of DUKE (1968), who noted textural similarities of the rock to terrestrial diabases, as supporting evidence for the formation of Shergotty in a shallow intrusive. Specifically, DUKE (1968)

presented two figures (Figs. 1, 2), which led him and others (SMITH and HERVIG, 1979; GRIMM and MCSWEEN, 1982) to suggest that, although pyroxene laths define a plane of layering (Fig. 1; DUKE, 1968), they appear to be randomly oriented in this plane (Fig. 2; DUKE, 1968). Figure 1 of DUKE (1968) is that of a hand specimen of Shergotty showing pyroxene layering, but the figure has an erroneous scale bar: It should be 1 cm instead of 4 cm (T. Thomas, pers. comm., 1990). Figure 2 of DUKE (1968) is a photomicrograph of Shergotty with a 12-mm field of view showing randomly oriented pyroxenes, and the figure caption reads "Section is in plane of layering, as shown by abundance of randomly oriented elongated prisms"; no other information regarding the orientation of the thin section relative to the hand specimen is given. SMITH and HERVIG (1979) and GRIMM and MCSWEEN (1982) interpreted this sentence to mean that the section was *intentionally* cut in the plane of layering, and displayed randomly oriented pyroxene laths. If this were the case, then they would have reason to argue for deposition of the pyroxene laths by settling onto the bottom of a magma body in the absence of any driving force, such as fluid motion in a flow and hence for formation of the rock in a shallow intrusive rather than in a lava flow. However, Duke (pers. comm., 1991) does not recall whether the thin section was cut in the plane of the layering or whether he simply inferred this from the random orientation of the pyroxene crystals. Note that examination by us of the original hand specimen

at the Smithsonian Institution could not resolve this issue since no cutting diagrams or residues from thin section preparation exist. We conclude that the presence of a foliation alone is not substantive evidence for the formation of Shergotty and Zagami by crystal settling in a magma chamber. It must be shown that an associated lineation does not exist. Our own work clearly documents the existence of at least a foliation in the fine-grained sample but cannot determine the existence of a lineation. As stated before, the presence of a foliation without an associated lineation would strongly favor an origin by crystal accumulation. Alternatively, the presence of an associated lineation would strongly favor a flow origin. A lineation could, in theory, form by convective flow in a magma chamber or in a lava flow on the surface. Clearly, carefully documented thin sections of known orientation need to be prepared from a large specimen to resolve this issue.

Cooling rate estimates: Thin, shallow intrusive or lava flow?

Evidence for formation of Zagami in the second stage in a near-surface environment comes from estimates of the cooling rate of the rock, based on pyroxene exsolution and plagioclase (maskelynite) size. BREARLEY (1991), based on widths of pyroxene exsolution lamellae of 300 Å, concludes that Zagami cooled at about 0.02°C/h through the temperature interval of 1100–950°C. He suggests that Zagami must therefore have originated in a lava flow significantly thicker than 10 m, or in a thin, shallow intrusive body such as a sill or a dike. We have attempted to determine the cooling rate of Zagami by an additional, independent method, in order to further characterize the physical setting of the crystallization of the rock during the second, near-surface stage (MCCOY et al., 1991).

The method that we applied is based on the experimental work of WALKER et al. (1976, 1978). These authors calibrated the grain size of groundmass plagioclase (i.e., the average width of the largest plagioclase laths) as a function of both cooling rate and distance from the edge of a magma body, and thus the method applies to the temperature range of plagioclase crystallization. To determine this parameter in Zagami, widths of the ten largest maskelynite grains were averaged. We found an average plagioclase width of 0.184 mm for the fine-grained material (UNM 991) and 0.318 mm for the coarse-grained material (UNM 994). From these measurements, we infer cooling rates of 0.1–0.5°C/h for these lithologies, using the data of WALKER et al. (1978), and thus crystallization 2–4 m from the edge of a magma body (WALKER et al., 1976). However, we caution that these numbers may be affected by uncertainties due to the fact that plagioclase appears to be a late-crystallizing phase that filled the residual areas between the pyroxenes, and thus plagioclase growth may have been inhibited. This suggests that Zagami may have cooled even slower than 0.1–0.5°C/h, and our cooling rates are therefore maximum estimates. Finally, it should be noted that the experiments of WALKER et al. (1978) were conducted with calcic plagioclase for eucritic compositions, not the intermediate plagioclase compositions of Zagami. It is uncertain what effect this compositional difference might have on the cooling rate estimates.

The cooling rates suggest crystallization of Zagami during the second stage in a near-surface environment, i.e., either in a thin, shallow intrusive or in a lava flow > 10 m in thickness (crystallization in a thick intrusion up to 1 km in thickness, as proposed by GRIMM and MCSWEEN (1982), is inconsistent with these calculations; although it should be noted that these authors had no supporting evidence for this thickness and used it as an upper limit for their calculations). We have no means to distinguish the two settings but are biased towards a lava flow origin because thick lava flows are common in the Tharsis region of Mars. For this area, SCHABER et al. (1978) report flow thicknesses between 5 and 20 m for the steeper shield slopes and between 20 and 65 m for the flatter terrains. MOUGINIS-MARK (1981) reports similar flow thicknesses from Arsia Mons in the Tharsis region. Thus, a lava flow setting for the second-stage cooling of Zagami and, by inference, for other shergottites as well is not inconceivable.

Crystallization sequence of pyroxenes

Since the Mg-rich pyroxene cores appear to have served as nucleation sites, it is likely that the Fe-rich pyroxene rims were the first phase to crystallize in the near-surface environment of the second stage. It is remarkable that the cores consist of augite and pigeonite in a ratio of 1.5 in the fine-grained and 2.2 in the coarse-grained lithology, whereas the rims are predominantly pigeonite (the ratio of pigeonite to augite rims is 12.3 in the coarse-grained lithology). This suggests that the system changed from crystallizing augite + pigeonite to crystallizing essentially only pigeonite from stage one to stage two. This is not the crystallization sequence normally predicted for this system. Fractional crystallization would not lead to pigeonite crystallizing after augite + pigeonite (JUSTER et al., 1989; LONGHI, 1991); although the phase relations are complex, and multiple crystallization paths may be possible. It is possible that kinetic effects may have suppressed the crystallization of augite, leading to the crystallization of only pigeonite at the start of the second magmatic stage. This type of crystallization behavior has been documented for Apollo 15 quartz-normative basalts (GROVE and RAUDSEPP, 1978), although kinetic effects are probably more important at cooling rates faster than Zagami experienced during the second magmatic stage. Alternatively, a shift in the phase boundaries in the augite-pigeonite-plagioclase plane of the basalt tetrahedron, which might lead to an expansion of the pigeonite field, can explain the observed crystallization sequence. This is illustrated schematically in Fig. 6, where crystallization may have begun during stage one in the pigeonite field (as indicated by the larger pigeonite cores) and progressed to the pigeonite-augite cotectic (dotted line), where both augite and pigeonite cores crystallized. A shift in the phase boundaries and expansion of the pigeonite field may have occurred as a consequence of the delivery of the magma to the near-surface environment in stage two, which would have resulted in crystallization of dominantly pigeonite rims around the homogeneous Mg-rich cores. The melt composition would then evolve towards the augite-pigeonite cotectic and, finally, to the eutectic, where plagioclase crystallization begins. In summary, the crystallization sequence of Zagami would have been pigeonite (?) → pigeonite + augite → pigeonite → pigeonite
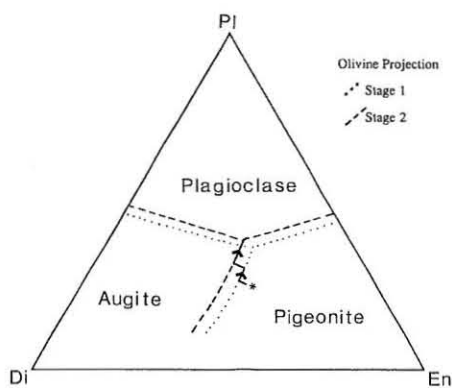
FIG. 6. Highly schematic projection from the olivine corner of the basalt tetrahedron onto the Di-En-Pl ternary plane. The crystallization path of Zagami is shown originating at the star (∗) and following the arrowed, solid line. The dotted lines are schematic representations of the phase boundaries during the first magmatic stage in the magma chamber. The solid lines indicate these boundaries during near-surface crystallization (second stage). Crystallization may have begun in the pigeonite field and moved to the augite-pigeonite cotectic during crystallization at depth, thus accounting for the homogeneous, Mg-rich pigeonite and augite cores. After transport to the near-surface during the second stage, the boundaries may have shifted and the pigeonite field became enlarged. Thus, only pigeonite crystallized, accounting for the Fe-rich rims consisting mostly of pigeonite. The composition of the melt continued to move to the augite-pigeonite cotectic and, finally, to the augite-pigeonite-plagioclase cotectic. This resulted in a crystallization sequence for Zagami of pigeonite → pigeonite + augite → pigeonite → pigeonite + augite → pigeonite + augite + plagioclase.

+ augite → pigeonite + augite + plagioclase. This unusual crystallization history might also explain the irregular shapes of the homogeneous Mg cores. Resorption of the cores during the second magmatic stage, as also suggested by BREARLEY (1991), might yield the irregular shapes, and small (10–20 μm) Fe-rich areas within the homogeneous Mg-rich cores might result from resorption in the third dimension, followed by rim crystallization. Alternatively, some small amount of solid-state diffusion may have obscured the original boundaries of the cores, although the rims are very steeply zoned, suggesting that the role of diffusional modification was small. If this were the case, Fe-rich pyroxene in the cores, especially around magmatic inclusions, might result from diffusive exchange. It should also be noted that the Fe-rich pyroxene might have crystallized from the magmatic inclusion itself, although we have not examined this possibility in detail. The cause of the speculated phase boundary shift upon extrusion is unknown. It may have resulted from a chemical change in the system, perhaps brought about by recharge of the shergottite magma chamber; although no definitive evidence exists for such a change. Alternatively, the phase boundary shift may have resulted from the large pressure change the system experienced upon eruption from the deep-seated magma chamber (≤1 kbar pressure) to the near-surface, potentially at an ambient pressure of ~7 mbar. To our knowledge, the effect such a large pressure change would have on the phase boundaries in this system is unknown, so we can only speculate on the origin of the peculiar changes in the pyroxene crystallization sequence.

Potential role of crystal settling in the near-surface environment (stage two)

We have also examined the role that crystal settling may have played in stage two. We used the same program we developed to model crystal settling in a magma chamber and estimated the settling of pyroxene cores in a lava flow during cooling from 1150–1000°C at a rate of 0.5°C/h. We assumed the same magma composition and abundance of crystals (20%) as in the earlier calculations; note that calculations using crystal sizes appropriate to the final pyroxene sizes in Zagami after overgrowth by Fe-rich rims, as suggested by SMITH and HERVIG (1979), did not yield significantly different results. We found that the Mg-rich cores during this entire temperature interval would only settle a total distance of 1.4 cm. This suggests that crystal settling and accumulation did not occur during crystallization in the near-surface environment of the second stage. Since crystal settling did not appear to play a major role in increasing the phenocryst content of Zagami during either magmatic stage, we conclude that Zagami resulted from crystallization of a liquid enriched in the "pyroxene" components relative to a basaltic liquid. This conclusion should not be all that surprising, since not all Martian lavas were necessarily basaltic. In fact, TREIMAN (1986) has invoked an ultramafic parental magma for the nakhlites.

CONCLUSION

We have conducted petrologic studies of new, large samples of the Zagami shergottite. Zagami experienced a two-stage magmatic history. The first magmatic stage occurred in a deep-seated (>7.5 km depth) magma chamber which experienced slow cooling. During this magmatic stage, both augite and pigeonite homogeneous Mg-rich cores crystallized and included amphibole-bearing melt inclusions. The phenocrysts were then entrained in the magma and emplaced at or near the surface in a thin intrusive or thick lava flow (at least 10-m thick) where cooling was rapid, and the rest of the rock crystallized. It does not appear that crystal settling played a significant role in either magmatic stage.

Editorial handling: D. W. Mittlefehldt

REFERENCES

ANTARCTIC METEORITE NEWSLETTER (1991), **14-2**, 19.
BOTTINGA Y. and WEILL D. F. (1970) Densities of liquid silicate systems calculated from partial molar volumes of oxide components. *Amer. J. Sci.* **269**, 169–182.
BREARLEY A. J. (1991) Subsolidus microstructures and cooling history of pyroxenes in the Zagami shergottite (abstr.). *Lunar Planet. Sci. XXII*, 135–136.

DAROT M. (1973) Methodes d'analyse structurale et cinematique. Application a'letude du massif ultrabasique de la Sierra Ronda. Ph.D. diss., Univ. of Nantes.

DELANEY J. S. and PRINZ M. (1989) Overview of some achondrite groups. In *Field and Laboratory Investigations of Meteorites from Victoria Land and the Thiel Mountains Region, Antarctica, 1982–1983 and 1983–1984.* (ed. U. B. MARVIN and G. J. MACPHERSON); *Smithson. Contrib. Earth Sci.* **28,** 65–79.

DUKE M. B. (1968) The Shergotty meteorite: Magmatic and shock metamorphic features. In *Shock Metamorphism of Natural Materials* (ed. B. M. FRENCH and N. M. SHORT), pp. 613–621. Mono Book Corp.

FUCHS L. H. (1969) The phosphate mineralogy of meteorites. In *Meteorite Research* (ed. P. M. MILLMAN), pp. 683–695. Reidel Publ.

GILBERT M. C., HELZ R. T., POPP R. K., and SPEAR F. S. (1982) Experimental studies of amphibole stability. In *Amphiboles: Petrology and Experimental Phase Relations.* (ed. D. R. VEBLEN and P. H. RIBBE) MSA.

GRIMM R. W. and MCSWEEN H. Y., JR. (1982) Numerical simulation of crystal fractionation in shergottite meteorites. *Proc. 13th Lunar Planet. Sci. Conf.,* pp. A385–A392.

GROVE T. L. and RAUDSEPP M. (1978) Effects of kinetics on the crystallization of quartz normative basalt 15597: An experimental study. *Proc. 9th Lunar Planet. Sci. Conf.,* pp. 585–599.

JAGOUTZ E. and WÄNKE H. (1986) Sr and Nd isotopic systematics of Shergotty meteorite. *Geochim. Cosmochim. Acta* **50,** 939–953.

JOHNSON M. C., RUTHERFORD M. J., and HESS P. C. (1991) Chassigny petrogenesis: Melt compositions, intensive parameters, and water contents of Martian (?) magmas. *Geochim. Cosmochim. Acta* **55,** 349–366.

JONES J. H. (1986) A discussion of isotopic systematics and mineral zoning in the shergottites: Evidence for a 180 m.y. igneous crystallization age. *Geochim. Cosmochim. Acta* **50,** 969–977.

JUSTER T. C., GROVE T. L., and PERFIT M. R. (1989) Experimental constraints on the generation of FeTi basalts, andesites, and rhyodacites at the Galapagos Spreading Center, 85°W and 95°W. *J. Geophys. Res.* **94,** 9251–9274.

LANGENHORST F., STÖFFLER D., and KLEIN D. (1991) Shock metamorphism of the Zagami achondrite (abstr.). *Lunar Planet. Sci.* XXII, 779–780.

LONGHI J. (1991) Comparative liquidus equilibria of hypersthene-normative basalts at low pressure. *Amer. Mineral.* **76,** 785–800.

MCBIRNEY A. R. (1984) *Igneous Petrology.* Freeman, Cooper, & Co.

MCCOY T. J., TAYLOR G. J., KEIL K., and NOLL P. D., JR. (1991) Zagami: Product of a two-stage magmatic history (abstr.). *Lunar Planet. Sci.* XXII, 867–868.

MCSWEEN H. Y., JR. (1985) SNC meteorites: Clues to Martian petrologic evolution. *Rev. Geophys.* **23,** 391–416.

MCSWEEN H. Y., JR., and JAROSEWICH E. (1983) Petrogenesis of the Elephant Moraine A79001 meteorite: Multiple magma pulses on the shergottite parent body. *Geochim. Cosmochim. Acta* **47,** 1501–1513.

MOUGINIS-MARK P. J. (1981) Late-stage summit activity of martian shield volcanoes. *Proc. 12th Lunar Planet. Sci. Conf.,* pp. 1431–1447.

MOUGINIS-MARK P. J., MCCOY T. J., TAYLOR G. J., and KEIL K. (1992) Martian parent craters for the SNC meteorites. *J. Geophys. Res.* (in press).

PEARCE T. H. (1987) The theory of zoning patterns in magmatic minerals using olivine as an example. *Contrib. Mineral. Petrol.* **97,** 451–459.

SCHABER G. G., HORSTMAN K. C., and DIAL A. L., JR. (1978) Lava flow materials in the Tharsis region of Mars. *Proc. 9th Lunar Planet. Sci. Conf.,* pp. 3433–3458.

SHAW H. R. (1972) Viscosities of magmatic silicate liquids: An empirical method of prediction. *Amer. J. Sci.* **272,** 870–893.

SMITH J. V. and HERVIG R. L. (1979) Shergotty meteorite: Mineralogy, petrography and minor elements. *Meteoritics* **14,** 121–142.

STOLPER E. and MCSWEEN H. Y., JR. (1979) Petrology and origin of the shergottite meteorites. *Geochim. Cosmochim. Acta* **43,** 1475–1498.

STÖFFLER D., OSTERTAG R., JAMMES C., PFANNSCHMIDT G., SEN GUPTA P. R., SIMON S. B., PAPIKE J. J., and BEAUCHAMP R. H. (1986) Shock metamorphism and petrography of the Shergotty achondrite. *Geochim. Cosmochim. Acta* **50,** 889–903.

TREIMAN A. H. (1985) Amphibole and hercynite spinel in Shergotty and Zagami: Magmatic water, depth of crystallization, and metasomatism. *Meteoritics* **20,** 229–243.

TREIMAN A. H. (1986) The parental magma of the Nakhla achondrite: Ultrabasic volcanism on the shergottite parent body. *Geochim. Cosmochim. Acta* **50,** 1061–1070.

TREIMAN A. H. and SUTTON S. R. (1991) Zagami: Trace element zoning of pyroxenes by synchrotron X-ray (SXRF) microprobe, and implications for rock genesis (abstr.). *Lunar Planet. Sci.* XXII, 1411–1412.

WALKER D., LONGHI J., KIRKPATRICK R. J., and HAYS J. F. (1976) Differentiation of an Apollo 12 picrite magma. *Proc. 7th Lunar Sci. Conf.,* pp. 1365–1389.

WALKER D., POWELL M. A., LOFGREN G. E., and HAYS J. F. (1978) Dynamic crystallization of a eucrite basalt. *Proc. 9th Lunar Sci. Conf.,* pp. 1369–1391.

ZUBER M. T. and MOUGINIS-MARK P. J. (1990) Constraints on magma chamber depth of the Olympus Mons volcano, Mars. In *MEVTV Workshop on the Evolution of Magma Bodies on Mars* (ed. P. MOUGINIS-MARK and J. HOLLOWAY); LPI Tech. Rpt. 90-04. pp. 58–59. Lunar Planetary Inst.